ELSEVIER

Physica C 274 (1997) 141–148

PHYSICA C

Raman spectroscopy and lattice-dynamics calculations of mixed layered copper-titanium oxides

M.V. Abrashev [a,b,*], C. Thomsen [a], V.N. Popov [c,b], L.N. Bozukov [b]

[a] *Institut für Festkörperphysik, Technische Universität Berlin, Hardenbergstrasse 36, 10623 Berlin, Germany*

[b] *Faculty of Physics, Sofia University, BG-1126, Sofia, Bulgaria*

[c] *Laboratoire de Physique des Solides, Université Pierre et Marie Curie, 4 Place Jussieu, 75252 Paris, France*

Received 24 September 1996

Abstract

We report micro-Raman spectra obtained from $R_2Ba_2Ti_2Cu_2O_{11}$ (R = Nd, Gd) and $Gd_2CaBa_2Ti_2Cu_2O_{12}$ ceramic samples. The analysis of the spectra was performed using the similarity between the investigated structures and related layered pure copper and titanium oxides. The assignment of the observed lines to definite atomic vibrations is supported by lattice-dynamics calculations, based on a shell model. The calculated frequencies for the IR-active modes are also presented. We stress that in contrast to $Gd_2CaBa_2Ti_2Cu_2O_{12}$, where the ceramics consist of optically anisotropic plate-like microcrystals, in the case of the quadruple perovskites $R_2Ba_2Ti_2Cu_2O_{11}$ the microcrystals are isotropic, probably due to the fine twinning, rendering it impossible to obtain polarized Raman spectra along different crystal directions.

Keywords: Copper-titanium oxides; Raman spectroscopy; Lattice dynamics

1. Introduction

It is well known that all high-T_c copper oxides have a layered structure containing CuO_2 sheets. Therefore, all newly discovered layered copper compounds are potential candidates for high-temperature superconductors and much attention is paid to their chemical variations in order to obtain optimal conditions for superconductivity. Undoubtedly, the interest in the layered copper compounds containing a rock-salt type insulating layer (the so-called "charge reservoir") is the greatest, because of the observed highest critical temperatures (all Pb-, Bi-, Tl- and Hg-compounds). Another type of layered structures successful with the respect to superconductivity is the oxygen deficient perovskite and its superstructures. The most investigated compounds of this type are $YBa_2Cu_3O_{7-x}$ (the "triple perovskite") and $(Sr,Ca)CuO_2$ (the "infinite-layer perovskite"). Unfortunately, most of the $(A,A')_n(Cu,B)_nO_{3n-x}$ (A and A′ are rare earth or alkaline earth elements; B - transition metal) perovskite superstructures are strongly disordered or ordered only in a 3-D copper framework [1].

The first member of the "quadruple perovskites" discovered (lattice constants $a_p \times a_p \times 4a_p$) is $La_2Ba_2Cu_2Sn_2O_{11}$ [2]. Recently, the isostructural Ti-analogs $R_2Ba_2Ti_2Cu_2O_{11}$ (R = La, Nd, Eu, Gd, Tb) with lattice parameters (Cu-O distances in the Cu-O plane) close to the high-T_c cuprates have been synthesized [3–5] (see Fig. 1). The crystal anisotropy

* Corresponding author. Fax: +49 30 314 27705.

PII S0921-4534(96)00657-0

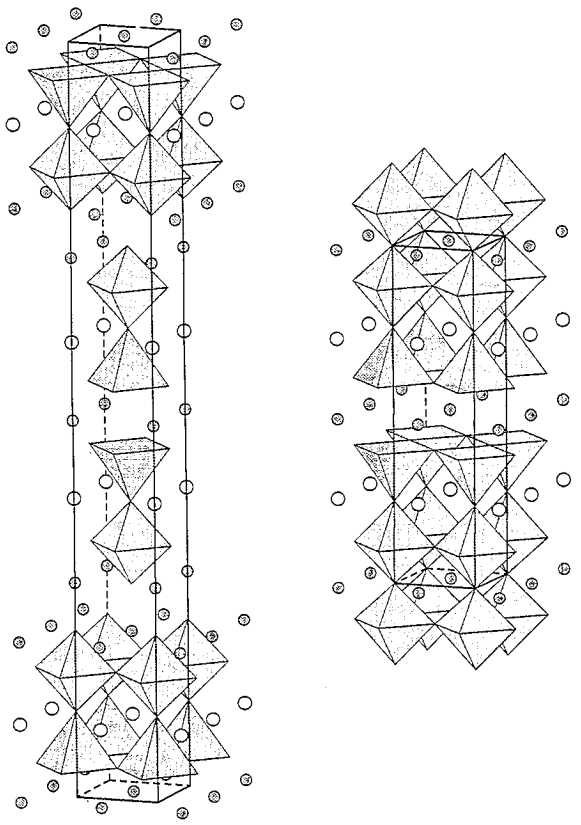

Fig. 1. Crystal structures and the unit cells of $Gd_2Ba_2Ti_2Cu_2O_{11}$ (right) and $Gd_2CaBa_2Ti_2Cu_2O_{12}$ (left). The dark circles are Gd (right) or (Gd,Ca) (left) atoms, the light circles are Ba atoms, Ti atoms are in the center of the oxygen octahedra, Cu atoms are in the centers of the bases of the oxygen pyramids.

of these compounds is weak and increases with decreasing ionic radius of the rare-earth element (for the La-compound the ratio is $c/a = 4.013$, where a and c are the parameters of the tetragonal lattice, for the Tb-compound - $c/a = 4.058$ [5]). An attempt to dope $Gd_2Ba_2Ti_2Cu_2O_{11}$ by substituting Gd with Ca leads to $Gd_2CaBa_2Ti_2Cu_2O_{12}$ [6] (see Fig. 1). In this structure an additional (Gd,Ca)-O layer is inserted between the Ti-O planes, leading to a body-centering of the lattice. Up to now superconductivity has not been observed in these type Cu-Ti compounds. One possible reason for this is the partial occupancy of Ti atoms in the Cu-O planes [7,8]. On the other hand, the attempts to prepare doped samples have not been successful yet [5,6,9].

In this paper we present and analyze micro-Raman spectra obtained on $R_2Ba_2Ti_2Cu_2O_{11}$ (R = Nd, Gd) (which we will abbreviate with R-2222) and $Gd_2CaBa_2Ti_2Cu_2O_{12}$ (Gd-3222) ceramic samples. From a Raman spectroscopic point of view it is interesting to investigate the changes of the vibrations arising from the Cu-O and Ti-O layers and their possible mixing, compared with similar vibrations in related compounds. The analysis of the Raman spectra of the homologous series $YBa_2Cu_{3+n}O_{7+n}$, ($n = 0, 1$) [10] and $Tl_mBa_2Ca_{n-1}Cu_nO_{2n+m+2}$, ($m = 1, 2$; $n = 1, 2, 3$) [11] shows that the differences in the modes from the common slabs in these compounds are very small and additional lines from the Raman-active modes appear only from the additionally inserted layers. This fact encouraged us to search for suitable compounds with well known Raman spectra for comparison. These are $YBa_2Cu_3O_{7-x}$ [12] and $Sr_{n+1}Ti_nO_{3n+1}$ (n = 1, 2, 3) [13]. On the other hand, in some layered cuprates that have two B_{1g} (or B_1) modes, there are indications for their strong mixing (e.g. $YBaCuFeO_5$ [14] and $(Bi,Cu)Sr_2(R,Ce)_2Cu_2O_{9-x}$ [15]). In these cases an assignment of the lines in the Raman spectra, based only on the comparison with the corresponding lines in the spectra of related compounds, is rather unreliable. In the investigated structures there are two B_{1g} modes (out-of phase vibrations along z of the oxygen atoms in the Cu- and Ti-planes) which, in principle, may mix. However, supported by lattice-dynamics calculations, we argue that in these structures the "layer by layer approach" for the assignment of the Raman lines is suitable.

2. Experimental

The R-2222 and Gd-3222 samples were prepared using a standard solid-state reaction technique following the procedure of Palacin et al. [5] and Fukuoka et al. [6]. Appropriate amounts of Nd_2O_3, Gd_2O_3, $BaCO_3$, $CaCO_3$, CuO and TiO_2 for the nominal compositions were mixed and heated in air several times for 24 h with intermediate grindings at temperatures from 950°C to 1030°C. The as-obtained materials were pressed into 1 g pellets and sintered at 1030°C for 48 h. A part of them was additionally heated to 1070°C (Gd-3222), 1100°C (Gd-2222) and up to 1300°C (Nd-2222). For the microscopic measurements the pellets were polished using 5 μm and 1 μm

diamond pastes and then ultrasonically cleaned in an ethanol bath.

The chemical content of the grains constituting the pellets, was determined by SEM-WDS microprobe (JEOL Superprobe 733). The results showed that the stoichiometry of the cations in the investigated structures is close to the nominal one. The lattice parameters were determined from the X-ray powder diffractograms obtained using a URD-6 powder diffractometer (Cu K_α radiation). They are: for Gd3222 - a = 3.890 Å, c = 35.50 Å; for Gd2222 - a = 3.901 Å, c = 15.76 Å; for Nd2222 - a = 3.950 Å, c = 15.80 Å. These values are close to those reported elsewhere [3,5,6]. All samples are monophasic.

The Raman spectra were measured using a Labram spectrometer equipped with an optical microscope. An 100x objective was used to focus the incident laser beam to a spot of 1÷2 μm diameter and to collect the scattered light in backward scattering geometry. A 632.8 nm He-Ne laser line was used for excitation. Additional measurements were done using a spectrometer Microdil 28 (Dilor) with 514.5 and 488 nm Ar^+ laser lines. The crystallographic directions of the investigated microcrystals in the case of the Gd-3222 sample sintered at 1070°C (these microcrystals have dimensions about 10 μm, larger than the laser spot) could be easily determined based on their regular shape (platelets parallel to the *ab* planes), optical anisotropy (the change of the color upon surface illumination with linearly polarized white light in different parallel and crossed polarizations) and the known polarization behavior of the Raman-active modes in compounds with similar structure [12]. The notations x, y, z, x', and y' will be used for the [100], [010], [001], [110] and [1$\bar{1}$0] crystallographic directions, respectively. In the case of R-2222, all attempts to identify crystallographic directions in the investigated polished grains were unsuccessful. The observed areas appeared optically isotropic, and all obtained Raman spectra were identical, independent of the polarization direction of the laser beam. This could be explained with the existence of a fine twinning on a scale lower than approximately 1 μm. The spectra obtained in these samples were identical for different sintering temperatures (for Nd-2222 up to 1300°C), as well.

3. Results and discussion

3.1. Classification of the Γ-point phonons

The R-2222 compounds crystallize in a tetragonal structure (space group $P4/mmm$, Z = 1). For R = Nd the lattice parameters are a = 3.9095 Å, c = 15.744 Å [7], for R = Gd, a = 3.8873 Å, c = 15.7335 Å [2]. The Gd-3222 structure belongs to space group $I4/mmm$, Z = 2, with a = 3.8939 Å and c = 35.4859 Å [6]. In Table 1 the atomic site symmetries and corresponding Γ-point phonon modes symmetries are given. Similarly to $La_{2-x}Sr_{1+x}Cu_2O_6$ [16], the cation positions in the rock-salt type layer and between the Cu-planes are occupied by Gd and Ca atoms in ratios 0.575/0.425 and 0.85/0.15, respectively [6]. The subscript for oxygen atoms indicates their place in the structure. For both structures O_{Cu} are oxygen atoms in the Cu-planes, O_{Ti} - in the Ti-planes, O_{Cu-Ti} - the apex oxygen for the CuO_5 pyramids. For R-2222, O_{Ti-Ti} are oxygen atoms between the Ti-planes, for Gd-3222, $O_{Gd/Ca}$ are oxygen atoms in the Gd/Ca rock-salt type layers. The A_{1g} and B_{1g} modes disscussed below are vibrations along the z axis, whereas the E_g modes are vibrations within the xy planes. The A_{1g} modes are allowed for parallel polarizations (xx, yy, zz), but forbidden for crossed polarizations (xy, xz, and yz) of incident and scattered radiation. The B_{1g} modes are allowed for the parallel (xx, yy) and crossed ($x'y'$) polarizations, but forbidden for zz, $x'x'$, xy, xz and yz configurations. The E_g modes are allowed only for xz ($x'z$) and yz ($y'z$). To identify the symmetry of the observed lines in the Raman spectra, we used seven type spectra from two type crystal surfaces: zz, xx and xz from an xz-oriented surface and xx, xy, $x'x'$ and $x'y'$ from an xy-oriented surface, respectively.

3.2. Calculations of the lattice dynamics

The model applied is a shell model with parameters derived as described in Ref. [17]. This model is appropriate for the perovskite-like oxides because, in accordance with their predominant ionicity, the interionic interactions are represented as sums of long-range Coulomb potentials and short-range (SR) potentials. The latter are chosen in the Born-Mayer-Buckingham form

Table 1
Site symmetry, irreducible representations and selection rules for R-2222 and Gd-3222 structures

$R_2Ba_2Ti_2Cu_2O_{11}$, $P4/mmm$, $Z = 1$			
Atom	Wickoff notation	Site Symmetry	Irreducible representations
R1	1c	D_{4h}	$A_{2u} + E_u$
R2	1d	D_{4h}	$A_{2u} + E_u$
Ba	2h	C_{4v}	$A_{1g} + A_{2u} + E_g + E_u$
Ti, Cu, O_{Cu-Ti}	2g	C_{4v}	$A_{1g} + A_{2u} + E_g + E_u$
O_{Ti-Ti}	1b	D_{4h}	$A_{2u} + E_u$
O_{Cu}, O_{Ti}	4i	C^v_{2v}	$A_{1g} + A_{2u} + B_{1g} + B_{2u} + 2E_g + 2E_u$
$Gd_2CaBa_2Ti_2Cu_2O_{12}$, $I4/mmm$, $Z = 2$			
Atom	Wickoff notation	Site Symmetry	Irreducible representations
Gd/Ca1	2b	D_{4h}	$A_{2u} + E_u$
Gd/Ca2, Ba, Cu, Ti, $O_{Gd/Ca}$, O_{Cu-Ti}	4e	C_{4v}	$A_{1g} + A_{2u} + E_g + E_u$
O_{Cu}, O_{Ti}	8g	C^v_{2v}	$A_{1g} + A_{2u} + B_{1g} + B_{2u} + 2E_g + 2E_u$
R-2222			Gd-3222
$\Gamma_{Raman} = 6A_{1g} + 2B_{1g} + 8E_g$			$\Gamma_{Raman} = 8A_{1g} + 2B_{1g} + 10E_g$
$\Gamma_{IR} = 8A_{2u} + 10E_u$			$\Gamma_{IR} = 8A_{2u} + 10E_u$
$\Gamma_{silent} = 2B_{2u}$			$\Gamma_{silent} = 2B_{2u}$
$\Gamma_{acoustic} = A_{2u} + E_u$			$\Gamma_{acoustic} = A_{2u} + E_u$
$A_{1g} \rightarrow \alpha_{xx} + \alpha_{yy}, \alpha_{zz}$ $B_{1g} \rightarrow \alpha_{xx} - \alpha_{yy}$			$E_g \rightarrow \alpha_{xz}, \alpha_{yz}$

$$V = a\exp(-br) - c/r^6. \quad (1)$$

Here a, b, and c are parameters, and r is the interionic separation. The ionic polarizability is also accounted for in the shell model using the simple picture of an ion as a point-charged core coupled with a force constant k to a charged massless shell with charge Y around it. The free ionic polarizability α is given by

$$\alpha = Y^2/k. \quad (2)$$

While the parameters for Ba, Cu, and Ti and the SR potentials for couples of these ions and oxygen ions were transfered unchanged, in the case of Gd and Ca in Gd-3222 some modifications of the model parameters were found necessary. These two kinds of ions substitute one another in the positions Gd/Ca1 and Gd/Ca2 and this makes it difficult to carry out the calculations of the phonon modes. It was accepted here to ascribe to the ions in positions Gd/Ca1 and Gd/Ca2 some averaged values of the model parameters. The ionic charges Z and the masses m were averaged proportionally to the corresponding occupation numbers. Further, the SR parameter a varies roughly as $Z^{1.2}$, and both the parameters a and b are inversely proportional to the interionic separation R [17]. In view of these results the values of the a and b parameters for the cations in positions Gd/Ca1 and Gd/Ca2 were determined. The attempts to use isotropic Gd/Ca2-O SR interactions have resulted in good correspondence with the experimental frequencies of the oxygen modes, but yielded unrealistically low values for the Gd/Ca2 and Ti A_{1g} modes and were hence abandoned. That is why, we reestimated the corresponding a and b parameters for each one of the three groups of oxygen ions coordinating the cation in position Gd/Ca2 (see Table 2).

Table 2
Shell model parameters. The O-O SR potential was taken from Ref. [18]

Ion	Z (|e|)	Y (|e|)	α (Å^3)	Ionic pair	a (eV)	b (Å^{-1})	c (eVÅ^6)
(Gd/Ca)1	2.71	1.7	0.7	(Gd/Ca)1-O	1535	2.854	0
(Gd/Ca)2	2.45	3.0	1.5	(Gd/Ca)2-$O_{Gd/Ca}$ (2.23Å)	1488	3.139	0
				(Gd/Ca)2-O_{Ti} (2.50Å)	1327	2.651	0
				(Gd/Ca)2-$O_{Gd/Ca}$ (2.78Å)	1194	2.518	0
Nd	2.85	1.7	0.7	Nd-O	1498	2.620	0
Ba	1.90	3.0	3.6	Ba-O	839	2.397	0
Cu	1.90	3.0	1.3	Cu-O	1400	3.550	0
Ti	3.80	2.0	0.2	Ti-O	2900	3.550	0
O	−1.90	-3.0	2.0	O-O	22764	6,711	20.37

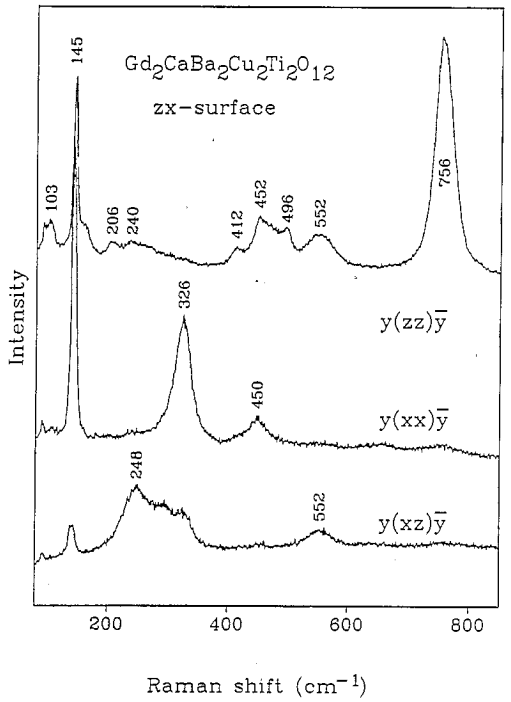

Fig. 2. Polarized Raman spectra obtained of a zx-oriented surface of a $Gd_2CaBa_2Ti_2Cu_2O_{12}$ microcrystal at room temperature. λ_L = 632.8 nm.

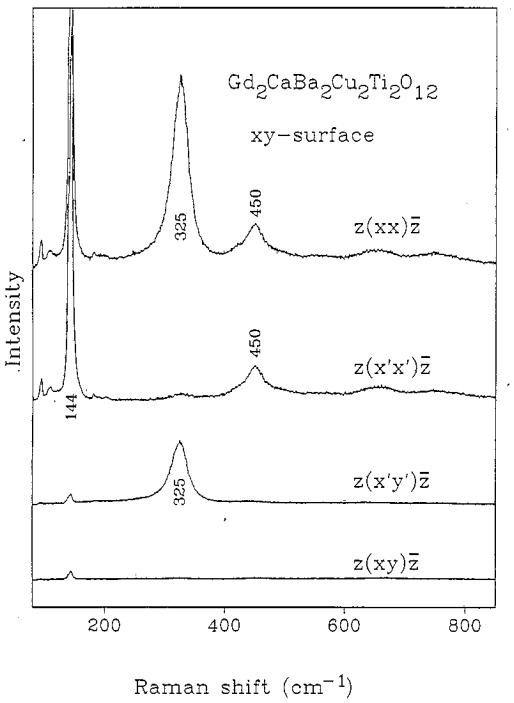

Fig. 3. Polarized Raman spectra obtained of a xy-oriented surface of a $Gd_2CaBa_2Ti_2Cu_2O_{12}$ microcrystal at room temperature. λ_L = 632.8 nm.

3.3. Gd-3222 Raman-active phonons

The spectra obtained from zx- and xy-oriented surfaces of Gd-3222 microcrystals are shown in Figs. 2 and 3. The frequencies of the lines compared with the calculated values and their assignment are presented in Table 3. The following lines have direct analogs in $YBa_2Cu_3O_{7-x}$ and other copper layered cuprates with two Cu-O planes per unit cell: the line at 103 cm^{-1} (Ba A_{1g} mode), the one at 145 cm^{-1} (Cu A_{1g} mode) and the one near 450 cm^{-1} (O_{Cu} A_{1g} in-phase mode). The assignment of the so-called "apex" mode (in this case the O_{Cu-Ti} A_{1g} mode) has to be done carefully, because its frequency varies strongly depending on the type of the cation in the insulating layer. This frequency may change from 460 cm^{-1} (in

Table 3
Experimental and calculated frequences (in cm^{-1}) and an assignment of the Raman-active modes

	Gd-3222		Nd-2222		Gd-2222	
Type	exp.	calc.	exp.	calc.	exp.	Assignment
A_{1g}	103	107	-	126	120	Ba
A_{1g}	145	149	145	148	145	Cu
A_{1g}	206	174				Gd/Ca2 (only in Gd-3222)
A_{1g}	240	219	-	255	-	Ti
A_{1g}	450	456	445	455	449	O_{Cu}
A_{1g}	496	502	-	560	-	O_{Ti}
A_{1g}	552	565				$O_{Gd/Ca}$ (only in Gd-3222)
A_{1g}	756	752	754	756	752	O_{Cu-Ti}
B_{1g}	325	323	308	314	330	O_{Cu}
B_{1g}	-	371	-	392	-	O_{Ti}
E_g	-	71	-	82	-	Ba
E_g	-	137				Gd/Ca2 (only in Gd-3222)
E_g	-	153	-	155	-	Cu
E_g	-	221	-	175	-	Ti
E_g	-	324	-	307	-	O_{Ti}
E_g	-	343	-	345	-	O_{Cu}
E_g	-	349	-	347	-	O_{Cu-Ti}
E_g	-	405				$O_{Gd/Ca}$ (only in Gd-3222)
E_g	-	506	-	506	-	O_{Cu}
E_g	-	641	-	610	-	O_{Ti}

$YBa_2Cu_3O_6$ [19]) to 590 cm^{-1} (in Hg-based superconductors [20]). However, in all cases this line is the strongest one in the spectra and visible mainly in zz polarization. In our spectra we have such line at 756 cm^{-1} (Fig. 2). The high frequency of the "apex" mode in this case may be explained with the smaller ionic radius and high valency (4+) of the adjacent Ti atom. A comparison with the Raman spectra of the isostructural Sr_2TiO_4 and La_2CuO_4 show such a hardening of the oxygen modes in the Ti-compound [13].

The remaining A_{1g} modes we compare with their analogs in $Sr_{n+1}Ti_nO_{3n+1}$ (n = 1, 2, 3). The line at 552 cm^{-1} we assign to the A_{1g} mode of $O_{Gd/Ca}$ atoms. The same oxygen mode in Sr_2TiO_4 is at 578 cm^{-1} (at 77K) [13]. The adjacent line at 496 cm^{-1} we assign to the A_{1g} in-phase mode of O_{Ti}. This mode occurs also in $Sr_3Ti_2O_7$ and $Sr_4Ti_3O_{10}$, but it was not discussed in Ref. [13]. We suggest that the line in Fig.2 of Ref. [13] near 500 cm^{-1} is similar to the O_{Ti} in-phase mode in our sample. This assignment is different from that by Graves et al. [21] in $Sr_4Ti_3O_{10}$ spectra, where this line was assigned as an E_g mode. The two weak peaks at 206 cm^{-1} and 240 cm^{-1} in zz polarization we tentatively assign to A_{1g} Gd/Ca and A_{1g} Ti modes. The frequency of the corresponding mode in Sr_2TiO_4 and La_2CuO_4 lies in the same spectral region (probably due to the nearly equal charge/mass ratios of La and Sr). The nearest calculated frequencies (at 174 cm^{-1} and at 219 cm^{-1}) are mixed Gd/Ca_2-Ti vibrations.

Out of the two B_{1g} modes, existing in Gd-3222, we observe only one line with this symmetry at 325 cm^{-1} (see Fig. 3). The lattice-dynamics calculations predicts a lack of mixing between these two modes. We assign the observed line to the B_{1g} O_{Cu} out-of-phase mode. Its frequency is in agreement with a similar frequency dependence on the type of the rare earth element [23,24] in the spectra of $RBa_2Cu_3O_7$. It further agrees with structural data for the dominant occupation of Gd in the position between the Cu-planes in Gd-3222 [6]. The weak line at 412 cm^{-1} in the zz spectra of Gd-3222 is of unclear origin. The narrow line at 94 cm^{-1} (observed in all spectra) is not connected with the investigated samples and originates from the Raman scattering of air.

It is difficult to assign the two structures observed in xz polarization to some of the 10 E_g modes. We remind only that in all layered cuprates the E_g lines have rather low intensities, compared to the A_{1g} lines and the structure between 248 and 330 cm^{-1} (with intensity comparable to some of the A_{1g} modes) could probably be assigned to modes originating from the Ti-O layer.

The calculated frequencies of the not Raman-active modes of both Gd-3222 and Nd-2222 structures are given in Table 4.

3.4. R-2222 Raman-active phonons

A typical spectrum obtained from Nd-2222 is presented in Fig. 4a. To analyze non-polarized spectra, containing 4÷5 lines from a structure with 16 Raman-active modes, is rather ambiguous. However, we argue that all observed lines excluding the line at 308 cm^{-1} (for Nd-2222) and at 330 cm^{-1} (for Gd-2222) are A_{1g} lines. Exploring the hypothesis of finely twinned grains in these ceramics, we compared the ratio of the intensities of the lines in cross ($I_\perp$) and parallel ($I_\parallel$) polarizations. This ratio in the case of randomly oriented scatterers must be 3/4 for B_{1g} and E_g modes and lower than 3/4 for A_{1g} modes

Table 4
Calculated frequences of the IR-active A_{2u}, E_u and the silent B_{2u} modes in Gd-3222 and Nd-2222

Gd-3222		Nd-2222		Gd-3222		Nd-2222	
A_{2u}(TO)	A_{2u}(LO)	A_{2u}(TO)	A_{2u}(LO)	E_u(TO)	E_u(LO)	E_u(TO)	E_u(LO)
63	81	55	83	76	77	78	79
150	150	151	151	117	118	118	118
182	184	177	177	189	190	188	190
229	239	212	217	215	229	190	201
321	446	330	445	321	333	266	316
527	531	520	529	344	348	342	345
532	587	619	657	348	370	346	383
712	754	702	756	513	555	383	484
				640	691	509	551
B_{2u}		B_{2u}		634	686	616	678
194		218					
372		375					

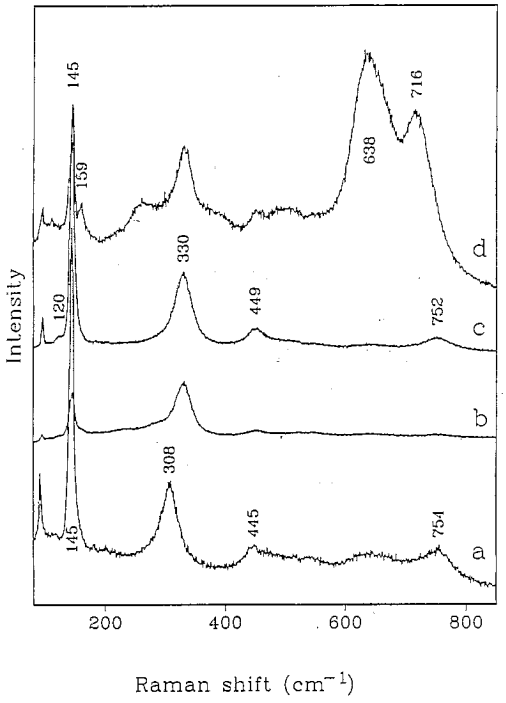

Fig. 4. (a) Nonpolarized Raman spectrum of $Nd_2Ba_2Ti_2Cu_2O_{11}$ grain. (b), (c) Polarized Raman spectra of $Gd_2Ba_2Ti_2Cu_2O_{11}$ grain in crossed and parallel polarization, respectively. (e) Nonpolarized spectrum of $Gd_2Ba_2Ti_2Cu_2O_{11}$ grain with probably distorted or disordered structure. λ_L = 632.8 nm.

(1/3 for an A_{1g} mode with $\alpha_{xx} = \alpha_{yy} \ll \alpha_{zz}$; 1/8 for A_{1g} mode with $\alpha_{xx} = \alpha_{yy} \gg \alpha_{zz}$; and ≈ 0 for an A_{1g} mode with $\alpha_{xx} = \alpha_{yy} \approx \alpha_{zz}$) [22]. Because of the finite number of clusters in the laser spot, optical phenomena connected with the presence of crystal faces, polarization leakage, the weak intensity of some lines, etc., it is difficult to obtain reliable results for this ratio for all the lines. However, a comparison of experimental ratio of the 308 cm^{-1} (330 cm^{-1} in Gd-2222) line with the ratio of all other lines suggests their A_{1g} symmetry (see Figs. 4b and 4c). Moreover, we can explore the similarity between the Gd-3222 and R-2222 structures. Therefore we assign the lines at 120 cm^{-1}, 145 cm^{-1}, 449 cm^{-1} (445 cm^{-1}) and 752 cm^{-1} (754 cm^{-1}) in Gd-2222 (Nd-2222) to Ba-, Cu-, O_{Cu}- and O_{Cu-Ti}-modes, respectively. All these lines have analogs with close frequencies in Gd-3222. This assignment is in accordance with the calculated frequencies of these modes in Nd-2222 as well. The high $I_\perp/I_\parallel$ ratio of the line at 308 cm^{-1} in Nd-2222 (330 cm^{-1} in Gd-2222) suggest its B_{1g} symmetry. The frequency shift depending on the type of rare earth (the distance between two oxygens from two adjacent Cu-O layers) is the same as for the similar B_{1g} mode in $RBa_2Cu_3O_{7-x}$ series [23,24].

After numerous checks of different grains in the R-2222 ceramics we have obtained in some cases a different type of spectra, one of them being displayed in Fig. 4d. In these spectra there are additional lines at

159 cm^{-1}, 638 cm^{-1} and 716 cm^{-1}. From the apparent similarity (intermediate cases have also been observed but are not displayed) with the "true" spectra, in our opinion these spectra indicate regions on the sample surface with lattice distortions resulting in a larger elementary cell [5] or a larger Cu-Ti disorder.

Finally we comment on the lack of observed mixing between the two B_{1g} (and the similar B_{2u}) modes. A significant mixing between two modes of the same symmetry exists only when the distance between adjacent oxygen atoms on different crystal positions, is on the order of two ionic radii of oxygen (2.8÷3.0 Å). Then the mixing leads to two coupled vibrations (in-phase and out-of-phase motions of these atoms), one of them with a low (below 200 cm^{-1}) frequency. In our case the distance between O_{Cu} and O_{Ti} is 4.52÷4.58 Å and this makes their vibrations practically independent. Moreover, comparing the calculated frequencies of the B_{1g} and B_{2u} modes of O_{Cu} and O_{Ti} (see Tables 3, 4), it is seen that only the B_{2u} mode of O_{Cu} has a low frequency, whereas the frequencies of the B_{1g} and B_{2u} modes of O_{Ti} are nearly equal. In our opinion the reason for this is the same - the distance between two adjacent O_{Ti} along z is rather large (3.63 Å). This rough rule could be used for a qualitative prediction of the frequencies of these type modes even in relatively complex structures.

In summary, we have measured the Raman spectra of the layered $R_2Ba_2Ti_2Cu_2O_{11}$ (R = Nd, Gd) and $Gd_2CaBa_2Ti_2Cu_2O_{12}$. The assignment of the observed lines is supported by lattice-dynamics calculations based on a shell model. Predictions for the frequencies of the IR-active modes were made. It is suggested that the "layer by layer approach" and a comparison with spectra of similar Cu- and Ti- structures is useful for a successful analysis of the spectra of more complex compounds.

Acknowledgements

We thank M. N. Iliev for his encouragment and S. Valkanov for the electron microprobe measurements. One of us (M.V.A.) acknowledges the financial support from the Alexander von Humboldt Foundation (Bonn, Germany) and thanks the Institut für Festkörperphysik (TU-Berlin) for its hospitality. This work is supported in part by Grant F530 (NIS 2241) of the Bulgarian National Science Fund.

References

[1] M.T. Anderson, K.B. Greenwood, G.A. Taylor and K.R. Poeppelmeier, Prog. Solid St. Chem. 22 (1993) 197.
[2] M.T. Anderson, K.R. Poeppelmeier, J.-P. Zhang, H.-J. Fan and L.D. Marks, Chem. Mater. 4 (1992) 1305.
[3] A. Gormezano and M.T. Weller, J. Mater. Chem. 3 (1993) 771.
[4] M.R. Palacin, A. Fuertes, N. Casan-Pastor and P. Gomez-Romero, Adv. Mater. 6 (1994) 54.
[5] M.R. Palacin, A. Fuertes, N. Casan-Pastor and P. Gomez-Romero, J. Solid State Chem. 119 (1995) 224.
[6] A. Fukuoka, S. Adachi, T. Sugano, X.-J. Wu and H. Yamauchi, Physica C 231 (1994) 372.
[7] R.A. Jennings and C. Graves, Physica C 235–240 (1994) 989.
[8] P. Gomez-Romero, M.R. Palacin and J. Rodrigues-Carvajal, Chem. Mater. 6 (1994) 2118.
[9] M.R. Palacin, N. Casan-Pastor, G. Krämer, M. Jansen and P. Gomez-Romero, Physica C 261 (1996) 71.
[10] E.T. Heyen, R. Liu, C. Thomsen, R. Kremer, M. Cardona, J. Karpinski, E. Kaldis and S. Rusiecki, Phys. Rev. 41 (1990) 11058.
[11] G. Burns, M.K. Crawford and F.H. Dacol, Physica C 179 (1990) 80.
[12] C. Thomsen, in: Light Scattering in Solids VI, eds. M. Cardona and G. Güntherodt (Springer Verlag, Heidelberg, 1991), p. 285.
[13] G. Burns, F.H. Dacol, G. Kliche, W. König and M.W. Shafer, Phys. Rev. B 37 (1988) 3381.
[14] Y.K. Atanassova, V.N. Popov, G.G. Bogachev, M.N. Iliev, C. Mitros, V. Psycharis and M. Pissas, Phys. Rev. B 47 (1993) 15201.
[15] M.V. Abrashev, V.N. Hadjimitov, L.N. Bozukov and M.N. Iliev, Solid State Commun. 93 (1995) 563.
[16] P. Lightfoot, S. Pei, J.D. Jorgensen, X.-X. Tang, A. Manthiram and J.B. Goodenough, Physica C 169 (1990) 464.
[17] V.N. Popov, J. Phys.: Condens. Matter 7 (1995) 1625.
[18] C.R.A. Catlow, W.C. Mackrodt, M.J. Norgett and A.M. Stoneham, Phil. Mag. 35 (1977) 177.
[19] R. Feile, Physica C 159 (1989) 1.
[20] M.C. Krantz, C. Thomsen, Hj. Mattausch and M. Cardona, Phys. Rev. B 50 (1994) 1165.
[21] P.R. Graves, S. Myhra, K. Hawkins and T.J. White, Physica C 181 (1991) 265.
[22] G. Herzberg, in: Molecular Spectra and Molecular Structure, Vol. II, (Van Nostrand Reinhold Company, New York, 1945), p. 245.
[23] H.J. Rosen, R.M. Macfarlane, E.M. Engler, V.Y. Lee and R.D. Jacowitz, Phys. Rev. B 38 (1988) 2460.
[24] M. Cardona, R. Liu, C. Thomsen, M. Bauer, L. Genzel, W. König, A. Wittlin, U. Amador, M. Barahona, F. Fernandez and R. Saez, Solid State Commun. 65 (1988) 71.